


Cite this: *RSC Sustainability*, 2024, 2, 179

Adsorption efficiency of crystal violet from the aqueous phase onto a carbonaceous material prepared from waste cotton and polyester

Fumihiko Ogata,^a Kazuki Sugimura,^a Noriaki Nagai,^a Chalermpong Saenjum,^{bc} Keiji Nishiwaki ^a and Naohito Kawasaki ^{*ad}

This research aims to evaluate waste cotton and polyester as effective potential adsorbents for the removal of crystal violet (CV) from aqueous phases. Carbonaceous materials (VCP1000 or VC1000) from waste cotton and polyester were prepared at different calcination temperatures, and their characteristics were assessed using scanning electron microscopy, pH_{pzc} , surface functional groups, and specific surface areas. The values of the parameters of VCP1000 or VC1000 were greater than those of other adsorbents. Additionally, adsorption experiments were performed in batch mode, and various parameters, including initial concentration, adsorption temperature, contact time, and pH, were demonstrated in this study. The amount of CV adsorbed onto VCP1000 and/or VC1000 was higher than those onto other VCP and/or VC adsorbents. The adsorption equilibrium of CV was achieved within 24 h. These data were fitted to the pseudo-second-order model (correlation coefficient: 0.991–0.995). The adsorption capacity increased with increasing adsorption temperatures ($7\text{ }^{\circ}\text{C} < 25\text{ }^{\circ}\text{C} < 45\text{ }^{\circ}\text{C}$). The adsorption isotherm data were fitted to both the Langmuir and Freundlich models as well. The adsorption of CV using VCP1000 or VC1000 was significantly influenced by pH under our experimental conditions. Finally, elemental distribution and binding energy analyses were conducted to elucidate the adsorption mechanisms of CV. The obtained results indicate that the adsorbed CV was presented onto the VCP1000 and/or VC1000 surface. Collectively, these obtained results show that VCP1000 or VC1000 holds promise for the removal of CV from aqueous phases.

Received 25th September 2023
Accepted 2nd November 2023

DOI: 10.1039/d3su00342f

rsc.li/rscsus

Sustainability spotlight

Goal 12, specifically focused on responsible consumption and production, aims to foster the development of innovative recycling technologies for reducing waste worldwide. In this study, we focus on textile products. The most produced fibers, such as cotton and polyester, were produced at 26 and 55 million tons, respectively. Interwoven cotton and polyester blends are extremely difficult to recycle and/or handle to reproduce new yarns. Hence, the development of value-added products, such as novel adsorbents derived from waste cotton and polyester for the purpose of removing CV from aqueous solutions, has the potential to make a substantial contribution to the realization of the SDGs and the purification of wastewater containing CV.

1 Introduction

Production of textiles clearly contributes to the rapid growth of economic expansion.¹ However, environmental pollution and the potential risks to human health from dye contamination are major concerns because large amounts of colored wastewater

are being released into water environments.² In addition, many serious environmental problems have been caused by wastewater containing harmful materials including dyes, owing to their carcinogenic properties and high toxicity.^{3–6} It is estimated that over tens of thousands of dyes and/or pigments are used industrially, corresponding to approximately 7×10^5 tons annually worldwide.⁷ According to estimates, an annual production of at least two hundred billion liters of dyeing wastewater has been recorded.⁸

Dyes possess intricate molecular structures and exhibit resilience against aerobic decomposition, remaining stable when exposed to light, heat, and oxidizing agents.⁷ Dyes can be categorized into three different classes: cationic, anionic, and nonionic dyes. In particular, cationic dyes are more dangerous than the other types. Crystal violet (CV) is a widely recognized

^aFaculty of Pharmacy, Kindai University, 3-4-1 Kowakae, Higashi-Osaka, Osaka, 577-8502, Japan. E-mail: kawasaki@phar.kindai.ac.jp

^bFaculty of Pharmacy, Chiang Mai University, Suthep Road, Muang District, Chiang Mai, 50200, Thailand

^cCenter of Excellence for Innovation in Analytical Science and Technology for Biodiversity-based Economic and Society (I-ANALY-S-T_B.BES-CMU), Chiang Mai University, Chiang Mai, 50200, Thailand

^dAntiaging Center, Kindai University, 3-4-1 Kowakae, Higashi-Osaka, Osaka, 577-8502, Japan



at 100 rpm to clarify the impact of pH on adsorption. The pH of the solution was measured using an F-73 digital pH meter (HORIBA, Japan).

The concentration of CV was measured through the following procedures. The equilibrium concentration of CV in the filtered sample solution after the adsorption reaction was determined using an ultraviolet-visible spectrophotometer UV-1280 (Shimadzu, Japan). The maximum absorption wavelength was 590 nm. The calibration curve was prepared over the range of 0.1–5.0 mg L⁻¹ and the correlation coefficient was determined to be over 0.999. Furthermore, the adsorbed CV was quantified by comparing concentrations before and after adsorption at various levels. All data are expressed as mean ± standard error ($n = 3-4$).

3 Results and discussion

3.1 Characteristics of the prepared adsorbents

The SEM images of the prepared adsorbents are shown in Fig. 1. The surface of VC remained significantly unchanged following calcination, whereas the surface of VCP clearly changed with calcination under the experimental conditions employed in our study. A previous study reported that polyester fiber was melted at approximately 250 °C.²⁷ Therefore, the surface of VCP adsorbent was smoothed as the calcination temperature increased.

Additionally, we could observe that VCP was clearly thermally decomposed at approximately 250 °C in this study (Fig. 2). These data supported the changes of the SEM image with calcination temperature.

In Table 1, the physicochemical properties of the adsorbents are presented. The value of pH_{pzc} increased with increasing calcination temperature. Additionally, the basic functional groups and specific surface areas also increased with increasing calcination temperature. Conversely, acidic functional groups exhibited different changes in the prepared adsorbents compared with other properties. FT-IR spectra of VCPs and VCs are shown in Fig. 3. O–H stretching vibration (3200–3550 cm⁻¹), O–H bending (850–1140 cm⁻¹), and C–O stretching vibration (1700–1720 cm⁻¹) were found in VCP and VC, whereas no characteristic peaks were found in calcined VCP and VC samples. In this study, the specific functional groups were not determined by FT-IR spectra. Therefore, further studies are necessary for determining the specific functional groups of carbonaceous materials prepared from waste cotton in detail.



Fig. 1 SEM images of the carbonaceous materials.



Fig. 2 TG-DTA analysis of VCP and VC.

3.2 Adsorption capacity of CV

Fig. 4 presents the amount of adsorbed CV using the prepared adsorbents. The amounts adsorbed onto VCP1000 and VC1000 were greater compared with those of other VCP and VC adsorbents. Previous research has indicated that factors, including functional groups, porous structures, micropores, and mesopores, can substantially influence the adsorption capacity and efficiency of selected adsorbents.²⁸⁻³⁰ Therefore, the correlation between the adsorbed CV amounts and the adsorbents' characteristics was evaluated. A high correlation was confirmed by a correlation coefficient of 0.930–0.969. In particular, the specific surface area is considered one of the factors that affect the adsorption capacity. Additionally, the high internal surface area of an adsorbent creates the high capacity needed for a successful purification process. In this study, this factor might be significantly related to the adsorption capacity of CV. Similar trends were observed in a previously reported study.³¹ These trends indicate that the surface characteristics of the prepared adsorbent are important factors for removing CV from aqueous phases.

3.3 Parameter effects on CV adsorption

The effects of the contact time on the adsorption of CV, using either VCP1000 or VC1000, are shown in Fig. 5. The amount of adsorbed CV increased with increasing adsorption time. The equilibrium concentration was achieved within 24 h under our experimental conditions.

Pseudo-first-order³² and pseudo-second-order models³³ are commonly applied to predict adsorption mechanisms. These models demonstrate the relationship between the amount of CV adsorbed as a function of time.³² We applied these models to analyze the data acquired from adsorption experiments, enabling us to establish kinetic parameters.

$$\ln(q_e - q_t) = \ln(q_e) - k_1 t \quad (1)$$

$$\frac{t}{q_t} = \frac{1}{k_2 q_e^2} + \frac{t}{q_e} \quad (2)$$

where q_e is the adsorption capacity at equilibrium (mg g⁻¹), q_t is the adsorption at time t (mg g⁻¹), k_1 is the rate constant of the pseudo-first-order model, and k_2 is the rate constant of the pseudo-second-order model.

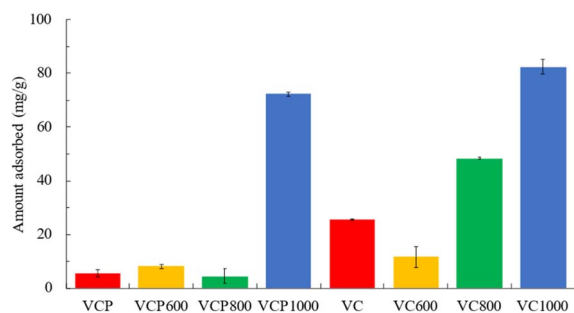


Table 1 Physicochemical properties of the adsorbents

Adsorbents	pH _{pzc}	Basic functional groups (mmol g ⁻¹)	Acidic functional groups (mmol g ⁻¹)	Specific surface area (m ² g ⁻¹)
VCP	6.72	0.00	0.03	N.D.
VCP600	6.60	0.08	0.26	583
VCP800	7.29	0.29	0.28	634
VCP1000	7.25	0.30	0.30	823
VC	6.42	0.00	0.11	N.D.
VC600	7.04	0.26	0.31	508
VC800	7.78	0.63	0.23	639
VC1000	9.89	0.82	0.17	660



Fig. 3 FT-IR spectra of VCPs and VCs.

Fig. 4 The amount of CV adsorbed onto adsorbents. Initial concentration: 50 mg L⁻¹, sample volume: 50 mL, adsorbent: 0.02 g, temperature: 25 °C, contact time: 24 h, 100 rpm.Fig. 5 The effect of contact time on the adsorption of CV onto VCP1000 or VC1000. Initial concentration, 100 mg L⁻¹; sample volume, 50 mL; adsorbent, 0.02 g; temperature, 25 °C; contact time, 10 and 30 min and 1, 1.5, 3, 6, 9, 12, 15, 18, 20, and 24 h, 100 rpm.

The data obtained for kinetic models are shown in Table 2. The correlation coefficient of the pseudo-second-order-model (0.991–0.995) was higher than that of the pseudo-first-order-model (0.941–0.963). Furthermore, the values of q_e (VCP1000, 99.4 mg g⁻¹; VC1000, 114.8 mg g⁻¹) estimated from experimental data also strongly align with the pseudo-second-order model (VCP1000, 103.5 mg g⁻¹; VC1000, 117.8 mg g⁻¹) compared with the pseudo-first-order model (VCP1000, 75.1 mg g⁻¹; VC1000, 70.4 mg g⁻¹). According to the results, CV adsorption onto VCP1000 or VC1000 may have occurred chemically.

Fig. 6 presents the adsorption isotherms of CV onto VCP1000 or VC1000. The amount of CV adsorbed increased with increasing adsorption temperatures (7 °C < 25 °C or 45 °C). The amount adsorbed at 45 °C slightly increased or did not significantly change compared with that at 25 °C. These patterns indicate that the saturated adsorption capacity of CV occurred within the temperature range of 25 °C to 45 °C.

The Langmuir and Freundlich isotherm models also provide valuable insights into adsorption mechanisms by estimating the adsorption of an adsorbate as a function of equilibrium concentration.³⁴ The Langmuir isotherm model assumes that adsorption takes place at specific homogeneous adsorption sites.³⁵ Meanwhile, at the same time, the Freundlich isotherm model is applicable for characterizing adsorption on heterogeneous surfaces.³⁶

$$\frac{1}{q_e} = \frac{1}{q_{\max}} + \left(\frac{1}{K_L q_{\max}} \right) \left(\frac{1}{C} \right) \quad (3)$$

$$\log q_e = \log K_F + \frac{1}{n} \log C \quad (4)$$

where q_e is the adsorption capacity at equilibrium (mg g⁻¹), q_{\max} is the maximum adsorption capacity (mg g⁻¹), K_L is the Langmuir model constant related to heat adsorption, and K_F and n are the Freundlich model constants designated as the adsorption capacity and adsorption intensity, respectively.

The Langmuir and Freundlich constants for the adsorption of CV are presented in Table 3. Under our experimental conditions, the Langmuir correlation coefficient ($r = 0.954$ – 0.996) and Freundlich correlation coefficient ($r = 0.940$ – 0.993) were found to be suitable for fitting the data. The value of q_{\max} using both VCP1000 and VC1000 increased with increasing adsorption temperatures. In addition, the value of K_F increased as the



Table 2 Kinetic parameters for CV adsorption onto VCP1000 or 1000

Adsorbents	$q_{e,exp}$ (mg g ⁻¹)	Pseudo-first-order model			Pseudo-second-order model		
		$q_{e,cal}$ (mg g ⁻¹)	k_1 (h ⁻¹)	r	$q_{e,cal}$ (mg g ⁻¹)	k_2 (mg g ⁻¹ h ⁻¹)	r
VCP1000	99.4	75.1	0.103	0.963	103.5	3.2×10^{-3}	0.991
VC1000	114.8	70.4	0.087	0.941	117.8	6.2×10^{-3}	0.995

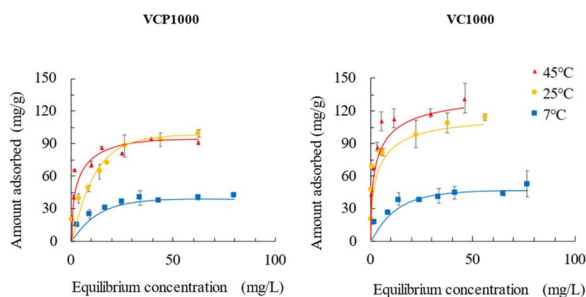


Fig. 6 The adsorption isotherms of CV onto VCP1000 or VC1000. Initial concentrations: 10, 20, 30, 40, 50, 60, 80, and 100 mg L⁻¹; sample volume: 50 mL; adsorbent: 0.02 g; temperatures: 7 °C, 25 °C, and 45 °C; contact time: 24 h, 100 rpm.

adsorption temperature increased, which indicated that the permeability of CV onto the adsorbent was enhanced by the greater contribution of kinetic energy at higher adsorption temperatures.¹¹

These observed trends were similar to the adsorption isotherm data presented in Fig. 6.

Furthermore, the occurrence of CV adsorption was readily observed when the $1/n$ value varied within the range of 0.1 to 0.5.³⁵ In this study, the value of the $1/n$ range was from 0.15 to 0.36, which indicated that CV was easily adsorbed onto VCP1000 or VC1000. In conclusion, the adsorption of CV onto the prepared adsorbents was controlled by multiple processes that involved both physical and chemical adsorption.³⁷

A previous study reported that the hydrogen bonding, electrostatic interaction, and π - π interactions were related to the adsorption mechanism of 4-nitroaniline onto MCM-48,³⁷ which indicates that the relationship between adsorbent surface roughness and contact angle is important to elucidate the adsorption mechanism in detail. In this study, the obtained results suggest that the properties of the VCP1000 and/or

VC1000 surface significantly affect the adsorption mechanism of CV from aqueous phases. As a result, we evaluated the binding energy and elemental distribution analysis both before and after the adsorption of CV (Fig. 7–9). The morphology of the VCP1000 and/or VC1000 surface slightly changed before and after adsorption (Fig. 7). Therefore, the CV was presented onto the adsorbent surface following the adsorption process.

Subsequently, carbon (C) and nitrogen (N) distribution intensities were measured. As shown in Fig. 8, the intensities of C and N, which were component elements of the CV structure, slightly increased after adsorption compared with those before adsorption (the warm and cold colors indicate high and low concentrations of CV, respectively). Additionally, the binding energies of C and N, which were slightly or not detected before adsorption, were clearly detected after the adsorption of CV in this study (Fig. 9). Collectively, the physicochemical characteristics of the adsorbent surface exhibited a notable correlation with CV adsorption.

Fig. 10 shows the effect of pH on the adsorption of CV onto VCP1000 or VC1000, the amount of adsorbed CV using VCP1000

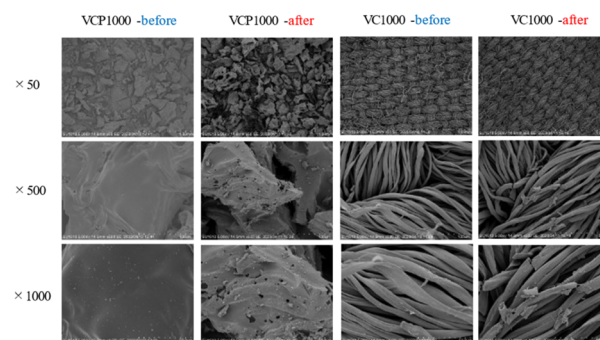


Fig. 7 The SEM images of VCP1000 and VC1000 before and after adsorption. Initial concentration, 100 mg L⁻¹; sample volume, 50 mL; adsorbent, 0.02 g; temperature, 25 °C; contact time, 24 h, 100 rpm.

Table 3 Langmuir and Freundlich constants for the adsorption of CV

Adsorbents	Temperature (°C)	Langmuir isotherm model			Freundlich isotherm model		
		q_{max} (mg g ⁻¹)	K_L (L mg ⁻¹)	r	$1/n$	$\log K_F$	r
VCP1000	7	43.9	0.17	0.996	0.31	1.08	0.961
	25	74.8	0.60	0.959	0.36	1.39	0.993
	45	76.6	2.75	0.960	0.23	1.61	0.944
VC1000	7	44.7	0.34	0.954	0.28	1.19	0.969
	25	97.2	3.83	0.957	0.15	1.81	0.981
	45	117.6	1.62	0.983	0.28	1.73	0.940



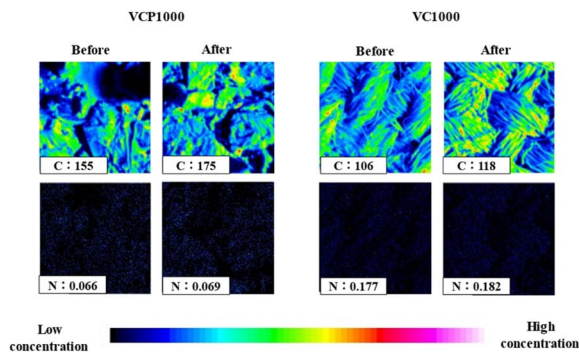


Fig. 8 The qualitative analysis of the adsorbent surfaces before and after adsorption.

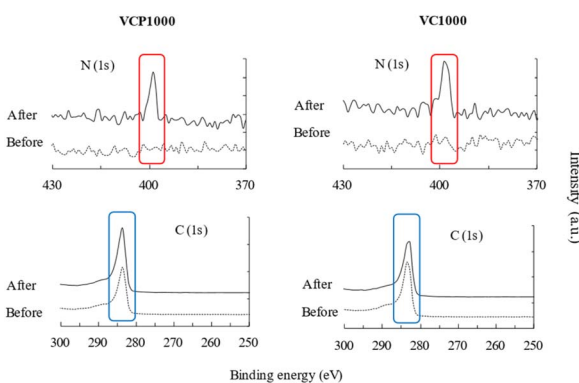


Fig. 9 The binding energies of the adsorbent surfaces before and after adsorption.

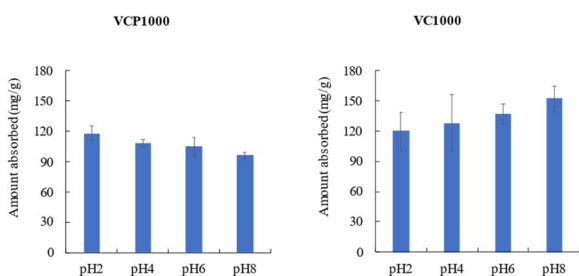


Fig. 10 The effect of pH on the adsorption of CV onto VCP1000 or VC1000. Initial concentration: 100 mg L⁻¹; pH in solution: 2, 4, 6, and 8; sample volume: 50 mL; adsorbent: 0.02 g; temperature: 25 °C; contact time: 24 h, 100 rpm.

slightly decreased or did not change. Meanwhile, a quite opposite trend was observed when using VC1000 under our experimental conditions. As mentioned, CV adsorption is possibly related to the physicochemical characteristics of the adsorbent surface. The interaction of CV with the prepared adsorbents depended on the solution pH. The adsorption capacity of CV changed with the changing surface charges of the prepared adsorbents from positive to negative.¹ For VCP1000, the values of pH_{pzc} , basic functional groups, acidic functional groups, and specific surface area were 7.25, 0.30 mmol g⁻¹, 0.30 mmol g⁻¹, and 823 m² g⁻¹, respectively, as shown in Table 1. According to our theory, alcoholic/phenolic hydroxyl groups (–OH) predominated among the functional groups in the adsorbent surface, with the remaining carbonyl groups (–COO) coming from polyester and cellulose (derived from cotton). pH_{pzc} generally strongly affects the adsorption capacity of VC.¹¹ However, the observed trend in adsorption capacity was not different from those previously reported in other studies.^{1,7} In other words, the adsorption capacity of CV was not significantly changed between pH 2 and pH 8. Therefore, physical properties, including the specific surface area, significantly affect the adsorption capacity of CV compared with other parameters in this study. However, further study is required to clarify the mechanisms by which VCP1000 adsorbs CV. In the case of VC1000, the pH_{pzc} , basic functional groups, acidic functional groups, and specific surface area were 9.89, 0.82 mmol g⁻¹, 0.17 mmol g⁻¹, and 660 m² g⁻¹, respectively (Table 1). In particular, the number of basic functional groups was approximately five times greater compared with the number of acidic functional groups. The value of pH_{pzc} was less than 9.89, implying that VC1000 was acidic and easily protonated. Additionally, the occurrence of excessive H⁺ (H₃O⁺) ions might have slightly caused the repulsion between the positively charged VC1000 and CV in the aqueous phase. Meanwhile, at high alkaline pH, the increase in HO⁻ ions caused deprotonation, which led to a gradually negative charge of VC1000 under our experimental conditions.^{1,11} Therefore, the amount of CV adsorbed increased with increasing solution pH.

3.4 Comparison of the CV adsorption with those of other reported adsorbents

Table 4 compares the CV adsorption capacity with those of other reported adsorbents.^{1,38–44} As shown in Table 4, VCP1000 and

Table 4 Comparison of the CV adsorption capacity with those of other reported adsorbents

Samples	Adsorption capacity (mg g ⁻¹)	pH	Temperature (°C)	Initial concentration (mg L ⁻¹)	Contact time (h)	Adsorbent (g L ⁻¹)	References
Charred rice husks	62.85	—	r.t.	50	24	1.0	Homagai <i>et al.</i> , 2022
Nascent rice husk	24.4781	—	25	500	24	16.7	Quansah <i>et al.</i> , 2020
Mango stone biocomposite	352.79	8.0	33	500	1	0.5	Shoukat <i>et al.</i> , 2017
Coconut husk	454.54	5.0	r.t.	400	3	1.0	Sultana <i>et al.</i> , 2022
Saw dust	37.83	—	23	100	5	4.0	Parab <i>et al.</i> , 2009
Coniferous pine bark	32.78	8.0	30	50	2	2.0	Ahmad, 2009
FCMFs	872	7.0	25	350	1	0.2	Baghdadi <i>et al.</i> , 2016
VCP1000	74.8	~5.0	25	100	24	0.4	This study
VC1000	92.8	~5.0	25	100	24	0.4	This study



- a potential low-cost adsorbent for the effective removal of toxic methyl violet 2B dye, *Appl. Water Sci.*, 2020, **10**, 243.
- 17 O. S. Bello, E. O. Alabi, K. A. Adegoke, S. A. Adegboyega, A. A. Inyinbor and A. O. Dada, Rhodamine B dye sequestration using Gmelina aborea leaf powder, *Heliyon*, 2020, **6**, e02872.
 - 18 H. A. Kiwaan, F. S. Mohamed, N. A. El-Ghamaz, N. M. Beshry and A. A. El-Bindary, Experimental and electrical studies of Na-X zeolite for the adsorption of different dyes, *J. Mol. Liq.*, 2021, **332**, 115877.
 - 19 S. Yadav, A. Yadav, N. Bagotia, A. K. Sharma and S. Kumar, Adsorptive potential of modified plant-based adsorbents for sequestration of dyes and heavy metals from wastewater – a review, *J. Water Process Eng.*, 2021, **42**, 102148.
 - 20 X. Dong, J. Yang, Y. Chen, X.-T. Zhen, Q.-Y. Wang, H. Zheng and J. Cao, Stigma maydis based plant adsorbent assisted miniaturized solid phase extraction of organophosphorus pesticides from crops, *Ind. Crop. Prod.*, 2020, **155**, 112832.
 - 21 The Fiber Year GmbH, *The fiber year 2019 – the survey on textiles & nonwovens*, 2019, available at, <https://thefiberyear.com/home/>, accessed July 15th, 2023.
 - 22 The Ellen MacArthur Foundation, *A new textiles economy: redesigning fashion's future*, 2017, available at, <https://www.ellenmacarthurfoundation.org/publications/a-new-textiles-economy-redesigning-fashions-future>, accessed July 15th, 2023.
 - 23 S. Haslinger, M. Hummel, A. Anghelescu-Hakala, M. Määttänen and H. Sixta, Upcycling of cotton polyester blended textile waste to new man-made cellulose fibers, *Waste Manage.*, 2019, **97**, 88–96.
 - 24 S. Haslinger, Y. Wang, M. Rissanen, M. B. Lossa, M. Tantt, E. Ilen, M. Määttänen, A. Harlin, M. Hummel and H. Sixta, Recycling of vat and reactive dyed textile waste to new colored man-made cellulose fibers, *Green Chem.*, 2019, **21**, 5598–5610.
 - 25 M. Mäkelä, M. Rissanen and H. Sixta, Machine vision estimates the polyester content in recyclable waste textiles, *Resour., Conserv. Recycl.*, 2020, **161**, 105007.
 - 26 H. P. Boehm, Chemical identification of surface groups, *J. Adv. Catal. Sci. Technol.*, 1966, **16**, 179–274.
 - 27 S. Tamada, K. Iida and T. Maruyama, Improvement of sound absorption characteristics by controlling the airflow resistance of surface layers, *The Journal of the INCE of Japan*, 2010, **34**(4), 317–324.
 - 28 P. C. C. Faria, J. J. M. Orfao and M. F. R. Pereira, Adsorption of anionic and cationic dyes on activated carbons with different surface chemistries, *Water Res.*, 2004, **38**, 2043–2052.
 - 29 L. Bulgariu, L. B. Escudero, O. S. Bello, M. Iqbal, J. Nisar, K. A. Adegoke, F. Alakhras, M. Kornaros and I. Anastopoulos, The utilization of leaf-based adsorbents for dyes removal: a review, *J. Mol. Liq.*, 2019, **276**, 728–747.
 - 30 D. Chen, L. Wang, Y. Ma and W. Yang, Super-adsorbent material based on functional polymer particles with a multilevel porous structure, *NPG Asia Mater.*, 2016, **8**, e301.
 - 31 N. Hassan, A. Shahat, A. El-Didamony, M. G. El-Desoukya and A. A. El-Bindary, Mesoporous iron oxide nano spheres for capturing organic dyes from water sources, *J. Mol. Struct.*, 2020, **1217**, 128361.
 - 32 A. T. Khadim, T. M. Albayati and N. M. C. Saady, Removal of sulfur compounds from real diesel fuel employing the encapsulated mesoporous material adsorbent Co/MCM-41 in a fixed-bed column, *Microporous Mesoporous Mater.*, 2022, **341**, 112020.
 - 33 S. Lagergren, About the theory of so-called adsorption of soluble substances, *Kongl. Vetensk. Acad. Handl.*, 1898, **24**, 1–39.
 - 34 Y. S. Ho and G. McKay, Pseudo-second order model for sorption processes, *Process Biochem.*, 1997, **34**, 451–465.
 - 35 N. Tahir, H. N. Bhatti, M. Iqbal and S. Noreen, Biopolymers composites with peanut hull waste biomass and application for crystal violet adsorption, *Int. J. Biol. Macromol.*, 2017, **94**, 210–220.
 - 36 I. Abe, K. Hayashi and M. Kitagawa, Studies on the adsorption of surfactants on activated carbons. I. Adsorption of nonionic surfactants, *Yukagaku*, 1976, **25**, 145–150.
 - 37 N. S. Ali, H. N. Harharah, I. K. Salih, N. M. C. Saady, S. Zendejboudi and T. M. Albayati, Applying MCM-48 mesoporous material, equilibrium, isotherm, and mechanism for the effective adsorption of 4-nitroaniline from wastewater, *Sci. Rep.*, 2023, **13**, 9837.
 - 38 Y. P. Gong, Z. Y. Ni, Z. Z. Xiong, L. H. Cheng and X. H. Xu, Phosphate and ammonium adsorption of the modified biochar based on Phragmites australis after phytoremediation, *Environ. Sci. Pollut. Res.*, 2017, **24**, 8236–8335.
 - 39 P. L. Homagai, R. Poudel, S. Poudel and A. Bhattarai, Adsorption and removal of crystal violet dye from aqueous solution by modified rice husk, *Heliyon*, 2022, **8**, e09261.
 - 40 J. O. Quansah, T. Hlaing, F. N. Lyonga, P. P. Kyi, S.-H. Hong, C.-G. Lee and S.-J. Park, Nascent rice husk as an adsorbent for removing cationic dyes from textile wastewater, *Appl. Sci.*, 2020, **10**(10), 3437.
 - 41 S. Shoukat, H. N. Bhatti, M. Iqbal and S. Noreen, Mango stone biocomposite preparation and application for crystal violet adsorption: a mechanistic study, *Microporous Mesoporous Mater.*, 2017, **239**, 180–189.
 - 42 H. Parab, M. Sudersanan, N. Shenoy, T. Pathare and B. Vaze, Use of agro-industrial wastes for removal of basic dyes from aqueous solutions, *Clean: Soil, Air, Water*, 2009, **37**(12), 963–969.
 - 43 R. Ahmad, Studies on adsorption of crystal violet dye from aqueous solution onto coniferous pinus bark powder (CPBP), *J. Hazard. Mater.*, 2009, **171**(1–3), 767–773.
 - 44 M. Baghdadi, A. Jafari and A. Pardakhti, Removal of crystal violet from aqueous solutions using functionalized cellulose microfibers: a benefit use of cellulosic healthcare waste, *RSC Adv.*, 2016, **6**, 61423.

